J. Earth Planet. Sci. Nagoya Univ., Vol. 42, 31 to 43, 1995

Late Permian CHIME ages of the Hida Gneiss and early Triassic age of the Mizunashi Granite in the Amo area of the Hida terrane, central Japan

Ibral, H. KHAN*, Kazuhiro SUZUKI, Ken SHIBATA** and Mamoru ADACHI****

Geoscience Laboratory, Geological Survey of Pakistan, Shehzad Town, P.O. Box 1461, Islamabad, 44,000, Pakistan
**Department of Earth and Planetary Sciences, Nagoya University, Nagoya 464-01, Japan*
(Received October 13, 1995 / Accepted December 15, 1995)

ABSTRACT

The CHIME (chemical Th-U-total Pb isochron method) dating of the Hida Gneiss, the Mizunashi Granite and a pegmatite vein have been carried out by precise microprobe analyses of monazite. The CHIME ages are 250.5±6.8 and 248.9±4.5 Ma for the Hida Gneiss, 236.8±4.7 Ma for the Mizunashi Granite and 180.1±2.5 Ma for the pegmatite vein. There is no age signature older than ca. 250 Ma even in the center of monazite grains; monazite ages date the first attainment of Hida metamorphism to the grade of monazite formation, the amphibolite facies. The emplacement of the Mizunashi Granite at 237 Ma may correspond to the peak metamorphism of the Hida Gneiss. The pegmatite vein in the Mizunashi Granite can be correlated in age with the Jurassic Funatsu granitic rocks.

INTRODUCTION

The Hida terrane located in the northern part of central Japan consists mainly of the Hida Gneiss, the Unazuki Schist and a series of granitoids. Although there has been extensive field, petrological and geochronological studies on rocks in the Hida terrane, a controversy exists on the age of the metamorphic and granitic rocks. Up to now, the authorized facts are: (1) among the granitoids, the Funatsu granitic rocks are the most widespread and were emplaced in Jurassic time (ca. 180 Ma, Shibata and Nozawa, 1984), (2) the Unazuki Schist formed in late Permian or early Triassic from upper Carboniferous to Permian sediments (Hiroi, 1981), and (3) the radiometric ages of the metamorphic rocks concentrate around 240 Ma (Shibata et al., 1970; Ota and Itaya, 1989).

The main point of arguments is whether the Hida Gneiss are of true Precambrian origin or not. Minato et al. (1965) pointed out that the Hida Gneiss bears the closest resemblance to the middle Precambrian Matenrei (Macho'llyong) System in the northeastern part of the Korean Peninsula. Sato et al. (1967) reported preliminary Rb-Sr model ages of 680-1200 Ma for the Gray

Granite that cuts the Hida Gneiss. These ages have never been confirmed, but the age data coupled with the mode of occurrence of the Gray Granite have long supported the idea that the Hida Gneiss is of polymetamorphosed Precambrian origin (e.g. Sato, 1968; Suwa, 1969, 1990, Suzuki, 1977; Hiroi, 1981). Subsequent Rb-Sr studies of the Gray Granite yielded whole-rock model age as old as ca. 1100 Ma (Shibata and Nozawa, 1986) and a whole-rock isochron age of 506 Ma (Shibata et al., 1989), whereas 230—250 Ma monazite and zircon ages were reported by the CHIME method (Suzuki and Adachi, 1991b); the timing of metamorphism and plutonism still remains controversial. This paper presents the results of CHIME (chemical Th-U-total Pb isochron method) dating on the Hida Gneiss and related Mizunashi Granite from the Amo area in the central Hida terrane.

GEOLOGICAL OUTLINE

Southwest Japan is divided into Inner and Outer Zones on the basis of their position with respect to the Median Tectonic Line (MTL in Fig. 1). The

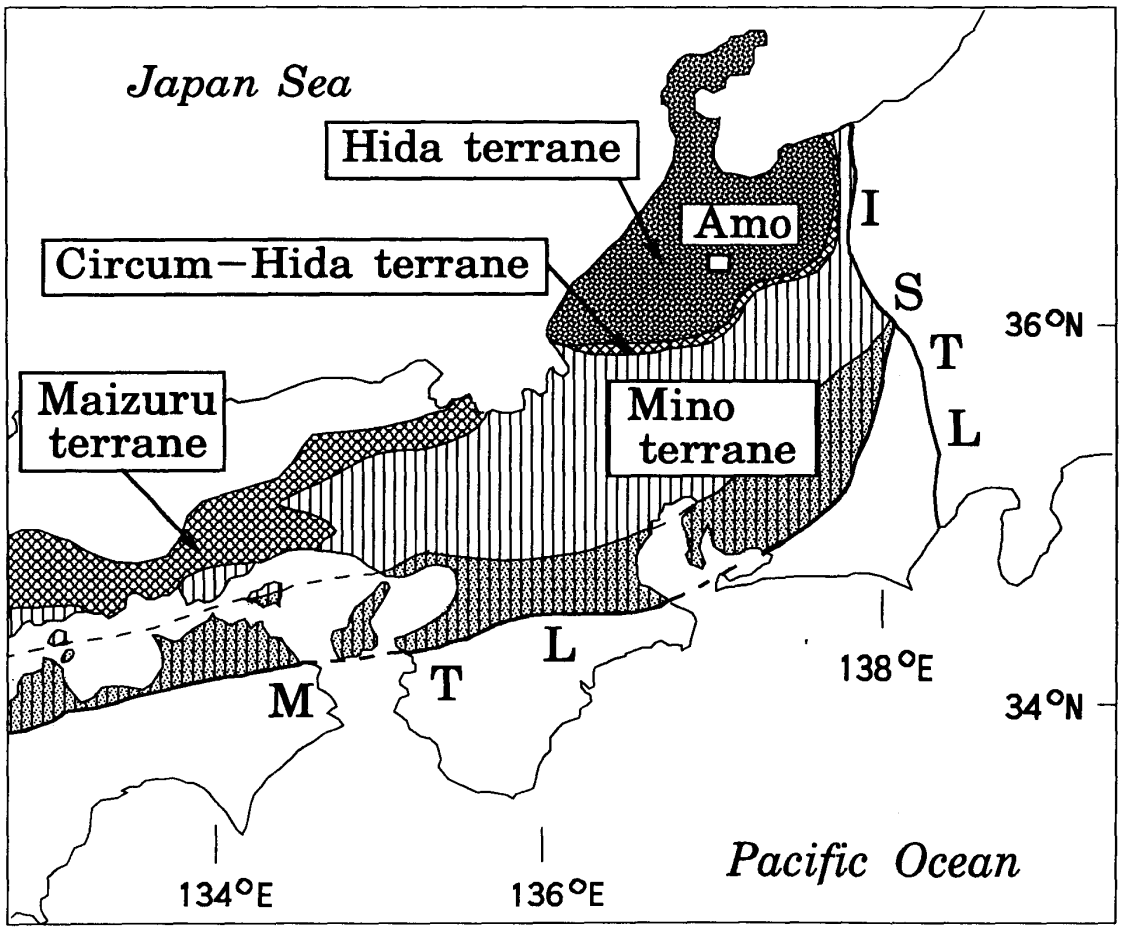

Fig. 1. Geologic framework of central Japan. MTL: the Median Tectonic Line, ISTL: the Itoigawa-Shizuoka Tectonic Line.

Inner Zone in central Japan consists of three pre-Tertiary terranes from north to south; (1) the Hida terrane of high T/P metamorphic rocks and granitoids, (2) the circum-Hida terrane of serpentinite melange with blocks of Paleozoic sediments and high P/T type metamorphic rocks, and (3) the Mino terrane of Jurassic sedimentary complex with disorganized blocks of Paleozoic limestone and greenstone and Triassic chert; the southern part of the Mino terrane is underlain by high T/P metamorphic rocks and granitoids, the Ryoke belt. The Hida terrane is underlain by the Hida Gneiss on the northwestern side, the Unazuki Schist on the southeastern side, and a variety of granitoids. They are covered with the late Jurassic to early Cretaceous Tetori Group, and Cenozoic sediments and volcanics.

Samples of the present study were collected from the Amo area. The geological configuration of the area is given in Fig. 2. The Hida Gneiss consists mainly of quartzo-feldspathic gneiss and crystalline limestone with subordinate amphibolite, pelitic gneiss and lime-silicate gneiss. The granite exposed in the western part of the study area is named as the Mizunashi Granite, and that in the southeastern part is correlatable with the Jurassic Funatsu granitic rocks (Nozawa et al., 1975).

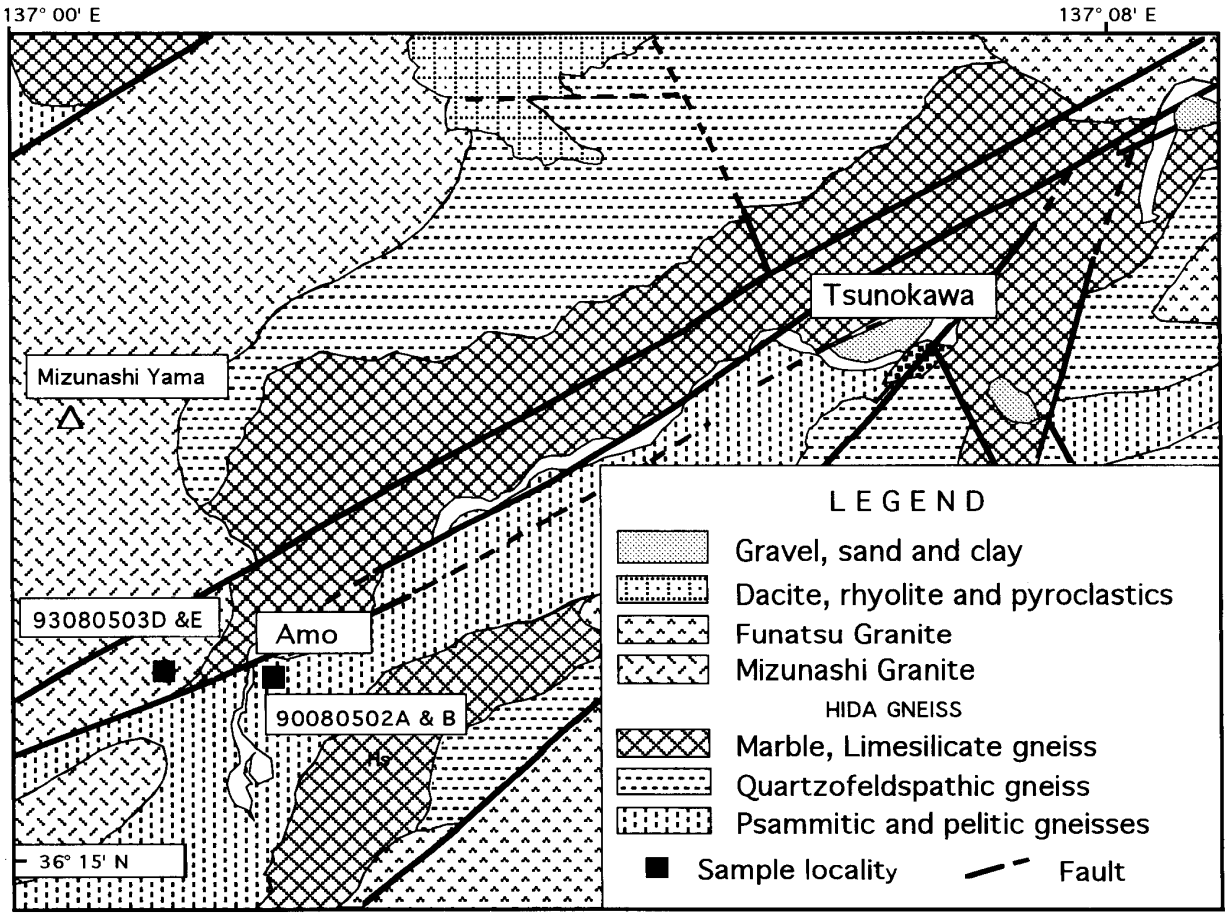

Fig. 2. Geologic map of the Amo area of the Hida terrane (simplified and modified from Nozawa et al., 1975), showing sample localities.

Two gneiss samples (Nos. 90080502A and 90080502B) were collected from thin pelitic layers intercalated with quartzo-feldspathic gneiss in an old graphite mine near Amo. The sample of Mizunashi Granite (93080503E) was collected from an outcrop about 1 km west of the mine, and sample 93080503D was collected from a pegmatite vein that cuts the Mizunashi Granite in the same outcrop as 93080503E. The gneiss samples are micaceous and consist essentially of biotite, muscovite, garnet, plagioclase and quartz with a substantial amount of graphite. Accessories include zircon, monazite, apatite and iron ores. The sample of the Mizunashi Granite is medium-grained hornblende-bearing biotite granite, and the pegmatite sample consists mainly of coarse-grained quartz and microcline with minor plagioclase, biotite and muscovite.

EXPERIMENTAL

Samples were crushed on a stamp mill. The size reduction was undertaken only to the extent necessary for disaggregation of monazite through periodic sieving to remove undersized (−60 mesh) particles before further reduction of oversized ones. Monazite and other heavy minerals were concentrated from each sieved sample by a pan. The concentrates were washed with dilute HCl and purified on an isodynamic magnetic separator. Monazite grains were hand-picked, mounted on a glass slide with Petropoxy 153 (Fig. 3A), and dried on a hot plate at 150°C. After covering with more Petropoxy 153 (Fig. 3B) and drying, the samples were polished with diamond paste until the grains were thinned approximately to half in thickness (Fig. 3C).

Monazites were analyzed on a JEOL JXA-733 electron microprobe provided with three wavelength-dispersive spectrometers (diameter of Rowland circle = 280 mm). The instrument operating conditions were 15 kV accelerating voltage, 0.15 μA probe current on Faraday cage, and 5 μm probe diameter. Intensities of ThMα, UMβ and PbMα lines only were measured using PET crystal. The background was measured at two optimum positions on both sides of each line peak position. Random error due to counting statistics was deduced by counting 300s at each line peak and two background. The line and background measurements were repeated twice, and the arithmetic average of the readings was taken. The comparison standards were euxenite provided by Smellie et al. (1978) for Th and U, and synthesized glass (56.17% PbO, 13.65% ZnO and 30.18% SiO_2, analyst: K. Hayashi) for Pb.

The Th, U and Pb intensities were converted into concentrations through the Bence-Albee correction method using an average monazite composition. The detection limit of Pb (as PbO) at 2σ confidence level is 0.007%, and the relative error in the Pb determination is around 8% at the 0.1% PbO level and much better for higher concentrations. The relative errors in the Th and U determinations are about 2% and 5%, respectively. Since the CHIME calculation has been described elsewhere (Suzuki and Adachi, 1991a,b, 1994; Adachi and Suzuki, 1992; Suzuki et al., 1991, 1992, 1994), the readers, if necessary, are recommended to refer to them.

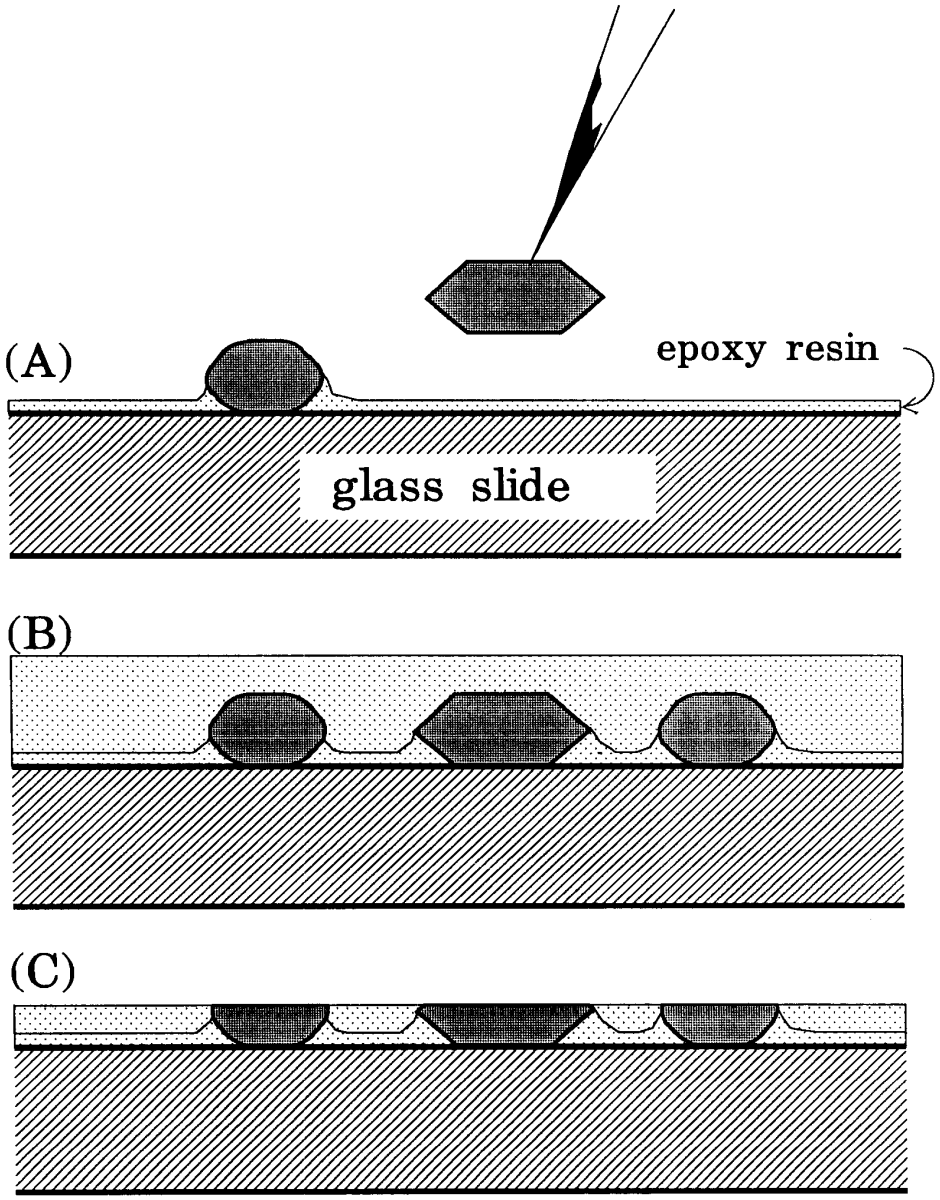

Fig. 3. Mounting of monazite grains on a glass slide (A), covering with Petropoxy 154 (B), and polishing with arundum and diamond paste (C).

RESULTS

The ThO_2, UO_2 and PbO analytical data of monazites together with apparent ages and calculated ThO_2* concentrations are listed in Table 1.

Hida Gneiss (Samples 90080502A and 90080502B)

A total of 95 spots on 29 monazite grains from sample 90080502A were analyzed. The ThO_2* content varies from 3.98 to 11.4%, and the PbO content from 0.044 to 0.121%. The apparent ages for most spots concentrate around 250 Ma, but those of spots 12-1 and 20-1 on metamict parts are about 200 Ma. The PbO-ThO_2* plots of 93 data are given in Fig. 4A. The regression line, having a

Table 1. Microprobe analyses of ThO_2, UO_2 and PbO of monazites from samples of the Hida Gneiss, Mizunashi Granite and pegmatite in the Amo area of the Hida terrane.

Grain#	ThO_2	UO_2	PbO	Age	ThO_2*
Hida Gneiss (sample 90080502A)					
M01-01	7.81	0.258	0.094	259	8.65
M01-02	7.95	0.265	0.094	254	8.81
M02-01	3.19	0.243	0.044	264	3.98
M02-02	5.38	0.264	0.064	245	6.24
M02-03	5.17	0.226	0.065	263	5.90
M02-04	5.25	0.253	0.062	241	6.07
M02-05	7.96	0.309	0.090	239	8.96
M02-06	4.58	0.231	0.054	240	5.33
M03-01	5.84	0.172	0.068	251	6.40
M03-02	5.97	0.149	0.072	263	6.45
M04-01	5.51	0.120	0.064	256	5.90
M04-02	5.61	0.150	0.067	262	6.10
M05	8.14	0.184	0.093	254	8.74
M06	6.40	0.226	0.077	257	7.13
M07	7.75	0.156	0.089	255	8.26
M08	7.73	0.154	0.088	253	8.23
M09	6.85	0.452	0.092	264	8.32
M10	7.14	0.205	0.085	257	7.80
M11	6.67	0.228	0.077	246	7.41
M12-01m	4.86	0.177	0.047	206	5.43
M12-02	5.48	0.196	0.068	263	6.12
M12-03	6.10	0.178	0.073	258	6.68
M12-04	6.33	0.159	0.070	242	6.85
M12-05	7.01	0.178	0.082	258	7.59
M12-06	7.44	0.168	0.087	260	7.99
M12-07	8.06	0.161	0.093	258	8.58
M12-08	7.27	0.182	0.081	244	7.86
M12-09	6.34	0.169	0.075	257	6.89
M12-10	8.90	0.168	0.103	260	9.45
M12-11	9.11	0.169	0.102	252	9.66
M12-12	8.82	0.169	0.099	250	9.37
M12-13	8.76	0.184	0.101	257	9.36
M12-14	8.75	0.167	0.093	239	9.29
M12-15	6.02	0.175	0.068	246	6.59
M12-16	8.62	0.163	0.097	253	9.15
M12-17	9.17	0.174	0.103	250	9.73
M12-18	8.94	0.189	0.102	252	9.55
M12-19	8.76	0.186	0.097	247	9.36
M12-20	6.80	0.198	0.081	259	7.44
M12-21	6.53	0.203	0.073	240	7.19
M12-22	7.41	0.259	0.085	244	8.25
M12-23	8.64	0.242	0.101	253	9.42
M12-24	8.76	0.250	0.107	266	9.57
M12-25	8.35	0.237	0.096	251	9.12
M12-26	8.59	0.237	0.102	260	9.36
M12-27	9.58	0.215	0.109	253	10.3
M12-28	7.13	0.267	0.082	242	8.00
M12-29	6.12	0.234	0.077	267	6.88
M12-30	6.24	0.269	0.078	259	7.11
M12-31	7.37	0.258	0.088	253	8.21
M12-32	8.56	0.219	0.098	250	9.27
M12-33	8.76	0.216	0.101	254	9.46
M12-34	8.13	0.211	0.095	257	8.81
M12-35	9.21	0.224	0.102	243	9.94
M12-36	8.78	0.188	0.104	264	9.39
M12-37	6.20	0.153	0.072	254	6.70
M12-38	6.10	0.210	0.076	265	6.78
M12-39	7.91	0.220	0.096	265	8.62
M12-40	9.86	0.183	0.110	249	10.5
M12-41	9.17	0.204	0.105	252	9.83
M12-42	8.39	0.212	0.097	255	9.08
M12-43	6.09	0.167	0.071	253	6.63
M12-44	5.80	0.180	0.065	243	6.38
M12-45	7.73	0.261	0.089	245	8.58
M13	6.85	0.219	0.083	259	7.56
M14	6.96	0.234	0.081	248	7.72
M15-01	6.34	0.201	0.075	254	6.99
M15-02	6.63	0.201	0.078	255	7.28
M15-03	5.73	0.267	0.070	253	6.60
M16-01	9.85	0.484	0.121	253	11.4
M16-02	9.28	0.442	0.113	251	10.7
M16-03	7.19	0.454	0.090	248	8.66
M17-01	5.31	0.130	0.060	247	5.73
M17-02	5.34	0.124	0.063	259	5.74
M18	6.11	0.166	0.072	258	6.65
M19	5.87	0.102	0.065	250	6.20
M20-01m	5.69	0.070	0.048	192	5.92
M20-02	6.04	0.123	0.073	270	6.44
M20-03	5.79	0.078	0.062	245	6.04
M21-01	6.06	0.133	0.071	261	6.49
M21-02	6.00	0.187	0.067	242	6.61
M22	6.05	0.180	0.068	242	6.63
M23	5.15	0.029	0.058	261	5.24
M24-01	6.90	0.392	0.085	246	8.17
M24-02	6.91	0.399	0.087	253	8.20
M24-03	5.96	0.281	0.074	257	6.87
M25	6.42	0.119	0.078	273	6.81
M26-01	6.74	0.157	0.073	240	7.25
M26-02	8.12	0.197	0.092	251	8.76
M26-03	7.04	0.196	0.083	258	7.68
M27	6.38	0.206	0.078	264	7.05
M28-01	6.39	0.155	0.073	250	6.89
M28-02	6.08	0.091	0.066	247	6.37
M29-01	8.37	0.226	0.098	257	9.10
M29-02	8.15	0.146	0.092	254	8.62
Hida Gneiss (sample 90080502B)					
M01-01	8.01	0.374	0.097	249	9.22
M01-02	8.16	0.637	0.108	249	10.2
M01-03	8.77	0.442	0.109	253	10.2
M01-04m	9.62	0.462	0.101	215	11.1
M01-05	8.17	0.308	0.095	245	9.17
M02-01	8.75	0.363	0.106	252	9.93
M02-02	9.27	0.392	0.110	247	10.5
M02-03	9.60	0.415	0.117	252	10.9
M02-04	9.48	0.442	0.115	249	10.9
M03-01	8.70	0.467	0.112	259	10.2
M03-02	8.30	0.458	0.103	249	9.78
M03-03	8.83	0.459	0.111	254	10.3
M03-04	7.21	0.554	0.093	244	9.01
M03-05	7.63	0.472	0.096	248	9.16
M04-01	8.73	0.583	0.113	251	10.6
M04-02	9.32	0.333	0.108	245	10.4
M04-03	8.22	0.484	0.104	251	9.79
M04-04	8.49	0.314	0.101	251	9.51
M04-05	8.18	0.450	0.098	240	9.64
M04-06	9.74	0.323	0.114	250	10.8
M04-07	9.82	0.315	0.116	253	10.8
M04-08	9.76	0.311	0.111	244	10.8
M04-09	9.65	0.353	0.114	250	10.8
M04-10	9.37	0.321	0.110	250	10.4
M04-11	8.69	0.520	0.110	250	10.4
M04-12	9.89	0.342	0.114	245	11.0
M04-13	9.77	0.307	0.112	246	10.8
M04-14	9.13	0.314	0.106	247	10.1
M04-15	8.14	0.270	0.096	252	9.02
M04-16	8.75	0.291	0.102	249	9.69
M04-17	9.56	0.309	0.114	255	10.6
M04-18	9.42	0.364	0.109	243	10.6
M04-19	9.71	0.284	0.111	247	10.6
M04-20	9.41	0.282	0.108	247	10.3
M04-21	9.07	0.357	0.109	252	10.2
M04-22	9.54	0.335	0.110	245	10.6
M04-23	8.97	0.271	0.103	247	9.85
M04-24	9.18	0.273	0.103	242	10.1
M04-25	8.91	0.250	0.099	241	9.72
M04-26	8.91	0.268	0.108	261	9.78
M04-27	10.2	0.315	0.119	250	11.2
M04-28	9.99	0.332	0.120	256	11.1
M04-29	9.63	0.310	0.113	251	10.6
M04-30	8.79	0.353	0.101	240	9.93
M04-31	8.71	0.338	0.103	248	9.81
M04-32	9.30	0.384	0.111	249	10.5
M04-33	10.3	0.432	0.125	253	11.7
M04-34m	7.98	0.058	0.063	182	8.17
M04-35m	7.79	0.139	0.062	178	8.24
M04-36	9.79	0.313	0.112	245	10.8
M04-37	9.37	0.265	0.109	252	10.2
M04-38	9.33	0.337	0.109	247	10.4
M04-39	8.87	0.334	0.107	254	9.95
M04-40	8.76	0.346	0.102	244	9.88
M04-41	9.37	0.364	0.110	246	10.5
M04-42	9.66	0.381	0.114	247	10.9
M04-43	10.0	0.400	0.121	253	11.3
M04-44	8.54	0.227	0.099	252	9.28
M04-45	9.47	0.322	0.109	245	10.5
M04-46	9.39	0.268	0.112	258	10.3
M04-47	8.86	0.335	0.106	252	9.95
M04-18	8.62	0.320	0.103	252	9.66
M04-49	8.87	0.333	0.105	249	9.95
M04-50	9.65	0.366	0.113	246	10.8
M04-51	9.67	0.365	0.114	248	10.9
M04-52	9.26	0.207	0.102	243	9.93
M04-53	8.83	0.320	0.105	252	9.87
M04-54	8.67	0.327	0.105	255	9.73
M04-55	8.64	0.310	0.102	250	9.65
M54-56	9.32	0.343	0.111	251	10.4
M04-57	8.95	0.419	0.112	257	10.3
M04-58	8.78	0.380	0.107	252	10.0

Table 1. (continued).

Grain#	ThO_2	UO_2	PbO	Age	ThO_2*
M04-59	8.69	0.338	0.101	244	9.79
M04-60	8.26	0.284	0.098	252	9.18
M04-61	8.93	0.325	0.106	251	9.98
M04-62	7.61	0.123	0.087	257	8.01
M05-01	10.6	0.474	0.128	248	12.1
M05-02	9.93	0.444	0.117	243	11.4
M05-03	8.98	0.381	0.110	254	10.2
M05-04	9.82	0.440	0.119	250	11.2
M05-05	9.85	0.475	0.119	247	11.4
M06-01	8.51	0.295	0.103	257	9.47
M06-02	9.43	0.294	0.111	253	10.4
M06-03	9.37	0.303	0.108	246	10.4
M06-04	9.12	0.291	0.107	251	10.1
M07-01	7.94	0.368	0.096	248	9.13
M07-02	7.89	0.359	0.094	245	9.05
M07-03	10.1	0.400	0.121	251	11.4
M07-04	10.6	0.418	0.124	245	12.0
M08-01	11.2	0.475	0.136	252	12.7
M08-02	10.1	0.528	0.124	248	11.8
M08-03	8.64	0.357	0.104	251	9.80
M08-04	10.7	0.432	0.126	246	12.1
M09-01	10.3	0.422	0.124	252	11.7
M09-02	8.63	0.386	0.107	256	9.88
M09-03	8.50	0.390	0.102	247	9.76
M09-04	10.4	0.421	0.125	252	11.8
M10-01	6.01	0.540	0.085	259	7.76
M10-02	5.53	0.500	0.075	248	7.15
M10-03	5.29	0.516	0.074	251	6.96
M10-04	5.72	0.477	0.078	254	7.27
M11-01	9.31	0.520	0.119	256	11.0
M11-02	9.96	0.537	0.123	248	11.7
M11-03	7.65	0.823	0.112	256	10.3
M11-04	10.8	0.531	0.134	253	12.5
M11-05	11.0	0.559	0.138	255	12.8
M12-01	6.24	0.639	0.089	253	8.31
M12-02	5.94	0.635	0.087	257	8.00
M12-03	5.45	0.675	0.081	250	7.64
M12-04	6.25	0.714	0.089	246	8.56
M13-01	7.83	0.395	0.097	251	9.11
M13-02	8.29	0.342	0.100	251	9.40
M13-03	9.29	0.356	0.109	247	10.4
M13-04	9.42	0.398	0.113	249	10.7
M13-05	9.57	0.416	0.115	249	10.9
M13-06	8.22	0.601	0.105	244	10.2
M14-01	9.92	1.37	0.149	245	14.4
M14-02	9.90	1.15	0.147	255	13.6
M14-03	10.9	0.725	0.139	248	13.3
M14-04	8.90	1.58	0.149	251	14.0
M14-05	10.3	0.495	0.126	250	11.9
M14-06	10.3	0.489	0.128	255	11.9
M15-01	9.34	0.363	0.113	254	10.5
M15-02	7.83	0.335	0.093	246	8.92
M15-03	8.43	0.311	0.101	253	9.44
M15-04	8.78	0.322	0.103	248	9.82
M16-01	9.53	0.295	0.111	250	10.5
M16-02	10.4	0.388	0.120	244	11.7
M17	8.93	0.352	0.108	253	10.1
M18	8.78	0.309	0.100	242	9.78
M19-01	8.35	0.368	0.101	250	9.54
M19-02	10.1	0.412	0.120	248	11.4
M20-01	7.64	0.263	0.089	248	8.49
M20-02	8.33	0.265	0.097	249	9.19
M21-01	7.12	0.280	0.085	250	8.03
M21-02	7.21	0.666	0.100	252	9.37
M22	9.31	0.447	0.115	253	10.8
M23	8.65	0.323	0.101	246	9.70
M24	9.40	0.358	0.114	255	10.6
M25	8.94	0.376	0.109	253	10.2
M26-01	7.87	0.287	0.092	247	8.80
M26-02	8.91	0.304	0.103	246	9.90
M27	9.08	0.322	0.107	250	10.1
M28	7.72	0.300	0.093	253	8.69
M29-01	8.65	0.404	0.106	251	9.96
M29-02	6.68	0.313	0.080	246	7.69
M30-01	9.04	0.258	0.105	251	9.88
M30-02	8.55	0.316	0.102	253	9.57
M30-03	7.46	0.703	0.101	245	9.74
M30-04	9.77	0.311	0.115	251	10.8
M31-01	9.62	0.351	0.117	257	10.8
M31-02	9.35	0.377	0.111	248	10.6
M31-03	9.11	0.444	0.111	250	10.5
M31-04	8.71	0.640	0.120	262	10.8
M31-05	10.0	0.399	0.118	246	11.3
M32-01	6.76	0.325	0.081	244	7.81
M32-02	9.36	0.383	0.111	247	10.6
M32-03	7.86	0.239	0.090	246	8.64
M33-01	5.05	0.346	0.066	251	6.17
M33-02	5.20	0.368	0.066	245	6.39
M33-03	5.18	0.362	0.069	255	6.35
M34-01	7.52	0.232	0.087	247	8.27
M34-02	8.21	0.228	0.096	254	8.95
M34-03	9.48	0.365	0.110	244	10.7
M34-04	8.46	0.367	0.102	249	9.65
M35-01	7.74	0.271	0.090	247	8.62
M35-02	8.15	0.217	0.093	247	8.85
M35-03	8.64	0.347	0.103	249	9.77
M36-01	6.84	0.606	0.091	245	8.80
M36-02	6.55	0.608	0.088	245	8.52
M36-03	6.37	0.621	0.091	255	8.38
M37-01	8.97	0.301	0.107	255	9.95
M37-02	9.35	0.309	0.106	242	10.4
M37-03	9.44	0.322	0.114	256	10.5
M37-04	9.24	0.309	0.109	251	10.2
M37-05	8.39	0.237	0.099	255	9.16
M37-06	9.78	0.362	0.116	250	11.0
M37-07	8.36	0.280	0.098	250	9.27
M37-08	9.47	0.356	0.110	245	10.6
M38-01	8.87	0.278	0.103	249	9.77
M38-02	8.85	0.272	0.102	248	9.73
M38-03	8.38	0.279	0.095	243	9.28
M38-04	8.59	0.271	0.100	249	9.47
M38-05	8.77	0.314	0.108	260	9.79
M38-06	8.49	0.382	0.100	242	9.73
M38-07	8.32	0.493	0.104	247	9.92
M38-08	9.02	0.255	0.102	245	9.85
M38-09	8.22	0.247	0.097	253	9.02
M39-01	7.44	0.366	0.091	248	8.63
M39-01	7.02	0.355	0.088	253	8.17
M39-03	6.78	0.338	0.083	248	7.88
M39-04	6.80	0.327	0.082	245	7.86
M39-05	6.85	0.329	0.082	245	7.92
M39-06	7.13	0.349	0.089	255	8.26
M39-07	7.15	0.349	0.085	242	8.28
M40-01	8.98	0.314	0.104	247	10.00
M40-02	8.48	0.336	0.104	257	9.57
M41-01	8.37	0.836	0.116	247	11.1
M41-02	8.34	0.833	0.117	250	11.0
M41-03	8.38	0.815	0.119	256	11.0
M41-04	8.39	0.810	0.114	245	11.0
M41-05	8.50	0.745	0.117	253	10.9
M41-06	8.48	0.745	0.116	251	10.9
M41-07	9.08	0.343	0.108	251	10.2
M41-08	8.81	0.459	0.108	248	10.3
M41-09	8.52	0.642	0.110	244	10.6
M41-10	8.53	0.717	0.114	247	10.9
M41-11	8.44	0.810	0.117	250	11.1
M41-12	8.66	0.768	0.117	248	11.2
M41-13	8.85	0.726	0.116	244	11.2
M12-14	9.97	0.475	0.121	248	11.5
M42-01	8.44	0.246	0.098	249	9.24
M42-02	8.17	0.240	0.097	256	8.95
M42-03	7.63	0.563	0.100	251	9.45
M43-01	8.27	0.361	0.099	248	9.44
M43-02	8.09	0.362	0.100	255	9.26
M43-03	8.02	0.371	0.096	246	9.22
M43-04	8.49	0.370	0.100	244	9.69
M43-05	8.71	0.259	0.101	251	9.55
M43-06	8.22	0.219	0.092	244	8.93
M43-07	8.02	0.388	0.096	244	9.28
M43-08	7.88	0.443	0.099	250	9.32
M44-01	8.79	0.658	0.114	246	10.9
M44-02	8.91	0.612	0.115	250	10.9
M44-03	8.15	0.654	0.112	257	10.3
M44-04	8.42	0.680	0.110	244	10.6
M44-05	8.38	0.640	0.111	251	10.5
M44-06	9.27	0.473	0.112	244	10.8
M44-08	9.69	0.419	0.114	245	11.0
M44-09	9.33	0.491	0.117	252	10.9
M45-01	8.49	0.269	0.103	260	9.36
M45-02	8.39	0.278	0.097	247	9.29
M45-03	8.48	0.245	0.099	252	9.27
M45-04	7.71	0.554	0.100	248	9.50
M45-05	7.67	0.520	0.099	250	9.36
M45-06	10.3	0.276	0.118	249	11.2
M45-07	11.0	0.244	0.123	247	11.8
M45-08	11.3	0.246	0.128	250	12.1
M45-09	8.35	0.852	0.115	245	11.1
M45-10	6.36	0.630	0.091	256	8.40
M45-11	6.74	0.667	0.095	252	8.90
M45-12	6.68	0.307	0.079	244	7.67
M46-01	5.43	0.399	0.070	245	6.72
M46-02	5.41	0.427	0.073	254	6.80
M46-03	5.07	0.381	0.067	252	6.31
M46-04	4.56	0.279	0.057	248	5.47
M46-05	5.27	0.389	0.069	249	6.53
M46-06	4.99	0.363	0.065	250	6.17

Table 1. (continued).

Grain#	ThO_2	UO_2	PbO	Age	ThO_2*
Mizunashi Granite (Sample 93080503E)					
M01-01	10.7	0.216	0.117	242	11.4
M01-02	6.72	0.121	0.072	238	7.11
M01-03	5.90	0.074	0.064	246	6.14
M01-04	3.16	0.069	0.035	247	3.38
M01-05	8.01	0.100	0.086	244	8.33
M01-06	7.55	0.071	0.078	238	7.78
M01-07	8.96	0.055	0.096	247	9.14
M02-01	8.62	0.128	0.092	241	9.03
M02-02	8.79	0.138	0.098	251	9.24
M02-03	8.78	0.133	0.093	239	9.21
M02-04	13.3	0.153	0.139	239	13.8
M02-05	9.27	0.139	0.097	236	9.72
M02-06	13.7	0.178	0.143	236	14.3
M02-07	12.2	0.181	0.132	245	12.8
M02-08	10.7	0.181	0.115	241	11.3
M03-01	10.4	0.304	0.112	233	11.4
M03-02	11.2	0.291	0.120	233	12.1
M03-03	12.9	0.295	0.143	243	13.9
M03-04	10.9	0.285	0.118	236	11.8
M03-05	11.0	0.305	0.124	245	12.0
M03-06	10.1	0.304	0.114	243	11.1
M04-01	10.1	0.093	0.105	237	10.4
M04-02	7.23	0.108	0.077	241	7.58
M04-03	10.2	0.122	0.106	235	10.6
M04-05	10.1	0.128	0.105	236	10.5
M05-01	9.76	0.106	0.100	235	10.1
M05-02	9.35	0.103	0.097	236	9.68
M05-03	12.1	0.140	0.127	239	12.6
M05-04	12.9	0.081	0.129	233	13.2
M05-05	12.5	0.078	0.129	238	12.8
M05-06	8.95	0.070	0.092	237	9.18
M06-01	6.35	0.023	0.064	234	6.42
M06-02	8.82	0.061	0.092	240	9.02
M06-03	7.62	0.022	0.078	239	7.69
M06-04	7.30	0.030	0.074	235	7.40
M06-05	11.5	0.026	0.116	236	11.6
M06-06	4.88	0.070	0.051	236	5.11
Pegmatite (sample 93080503D)					
M01-01	2.45	0.023	0.019	181	2.52
M01-02	2.07	0.016	0.018	196	2.12
M01-03	1.84	0.013	0.015	188	1.88
M02-01	2.49	0.035	0.019	176	2.60
M02-02	2.05	0.019	0.015	173	2.11
M02-03	1.84	0.017	0.015	181	1.90
M02-04	2.41	0.027	0.019	183	2.50
M02-05	2.46	0.018	0.020	189	2.52
M02-06	1.90	0.015	0.014	165	1.95
M03-01	2.84	0.030	0.022	178	2.94
M03-02	2.02	0.039	0.015	162	2.15
M03-03	1.95	0.034	0.016	188	2.06
M03-04	1.71	0.017	0.013	174	1.76
M03-05	1.86	0.020	0.014	168	1.92
M04-01	13.9	0.140	0.109	180	14.4
M04-02	15.1	0.185	0.115	174	15.7
M04-03	15.0	0.199	0.122	184	15.6
M04-04	17.5	0.160	0.136	178	18.0
M04-05	12.0	0.059	0.092	178	12.2
M04-06	31.1	0.294	0.244	180	32.0
M04-07	15.0	0.130	0.117	179	15.4
M05-01	4.56	0.026	0.034	174	4.64
M05-02	3.63	0.024	0.029	186	3.71
M05-03	3.70	0.051	0.028	172	3.86
M06-01	3.74	0.018	0.030	187	3.80
M06-02	1.58	0.022	0.014	195	1.65
M06-03	1.62	0.079	0.014	177	1.87
M07-01	2.62	0.014	0.019	164	2.66
M07-02	2.69	0.029	0.021	176	2.78
M08-01	2.79	0.021	0.021	171	2.86
M08-02	1.70	0.020	0.012	166	1.76
M08-03	1.67	0.023	0.013	176	1.74
M08-04	2.31	0.037	0.018	170	2.43
M09-01	2.61	0.021	0.021	185	2.68
M10-01	2.29	0.014	0.018	183	2.33
M10-02	3.08	0.025	0.024	180	3.16
M10-03	1.18	0.165	0.012	168	1.71
M10-04	4.38	0.138	0.038	188	4.82
M10-05	2.46	0.023	0.020	186	2.53
M10-06	4.44	0.024	0.034	178	4.52
M10-07	2.35	0.037	0.018	171	2.47
M10-08	4.95	0.108	0.041	183	5.30
M11-01	5.94	0.116	0.048	179	6.32
M11-02	3.10	0.030	0.026	188	3.20
M11-03	4.43	0.042	0.035	183	4.57
M11-04	2.99	0.025	0.024	182	3.07
M11-05	4.50	0.035	0.037	191	4.61
M11-06	4.09	0.038	0.030	169	4.21
M12-01	2.30	0.015	0.017	175	2.35
M12-02	2.07	0.037	0.016	171	2.19
M12-03	4.34	0.053	0.034	180	4.51
M12-04	5.29	0.083	0.043	182	5.56
M12-05	4.40	0.340	0.039	166	5.50
M12-06	7.49	0.059	0.059	180	7.68
M13-01	2.30	0.024	0.018	175	2.38
M13-02	3.20	0.013	0.025	181	3.24
M13-03	3.44	0.019	0.026	178	3.50
M13-04	4.74	0.030	0.036	177	4.84

slope of 0.0105 ± 0.0003 and an intercept value of 0.0007 ± 0.0023, yields an age of 250.5 ± 6.8 Ma (MSWD = 0.17).

A total of 248 spots on 46 monazite grains from sample 90080502B were analyzed. The ThO_2* content varies from 5.47 to 14.4% and the PbO content from 0.057 to 0.149%. The apparent ages are in the range between 240 and 261 Ma, but three spots (M01-04, M04-33 and M04-34) on metamict parts give much younger apparent ages of 200—180 Ma. The PbO-ThO_2* plots of 245 data are given in Fig. 4B. They are regressed with an isochron of 248.9 ± 4.5 Ma (MSWD = 0.13) with a slope of 0.0105 ± 0.0002 and an intercept value of 0.0005 ± 0.0019.

Mizunashi Granite (Sample 93080503E)

A total of 37 spots on transparent portions of 6 monazite grains were analyzed. Monazite contains 3.38 to 14.3% ThO_2* and 0.035 to 0.143% PbO. All data points are arrayed linearly on the PbO vs. ThO_2* diagram (Fig. 5A), yielding isochron (MSWD = 0.12) of 236.8 ± 4.7 Ma with a slope of 0.0100 ± 0.0002 and an intercept value of 0.0009 ± 0.0020.

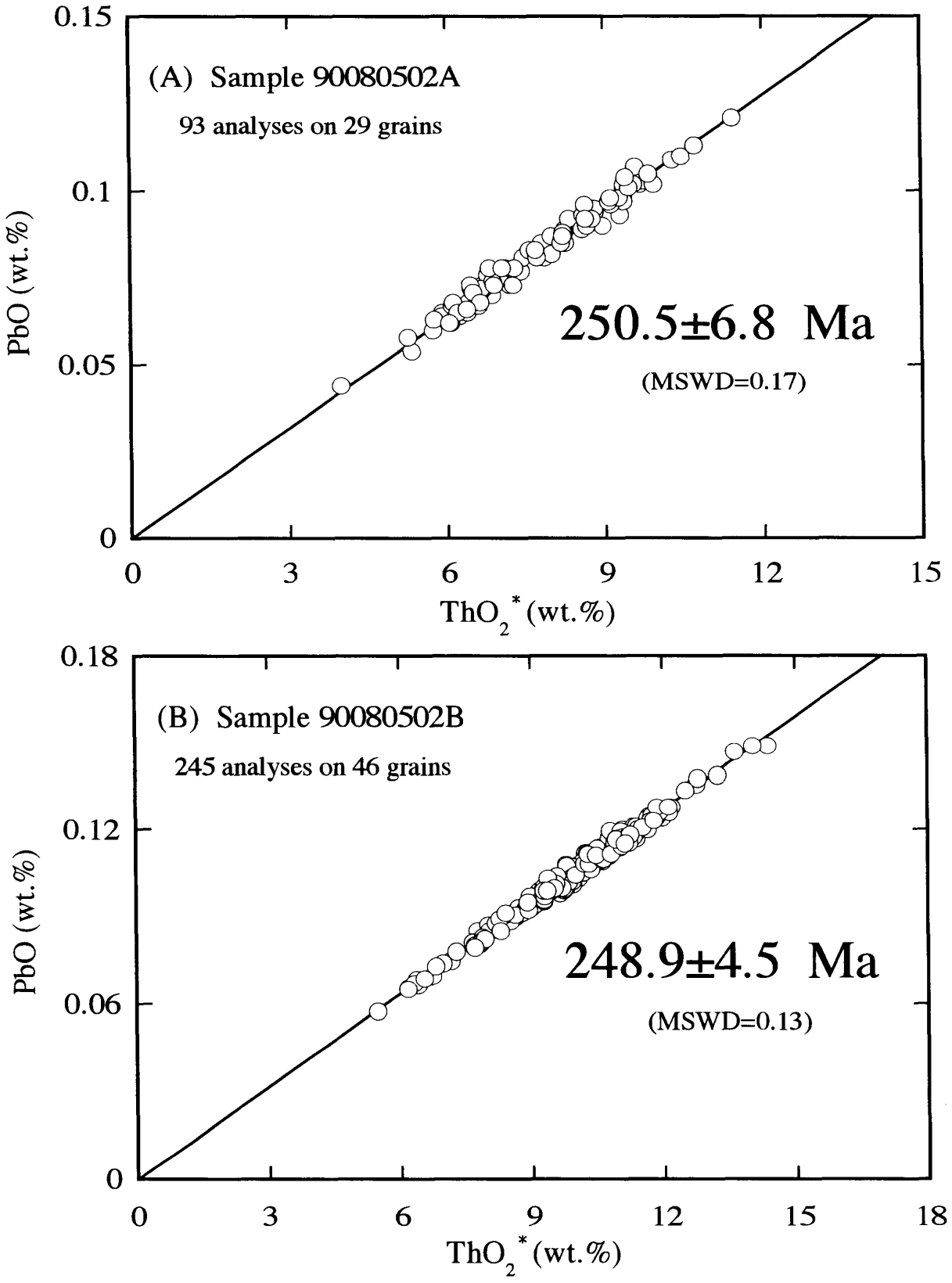

Fig. 4. Plots of PbO vs. ThO_2^* of monazite grains from sample 90080502A (A) and from sample 90080502B (B). The error given to the age calculation is of 2σ.

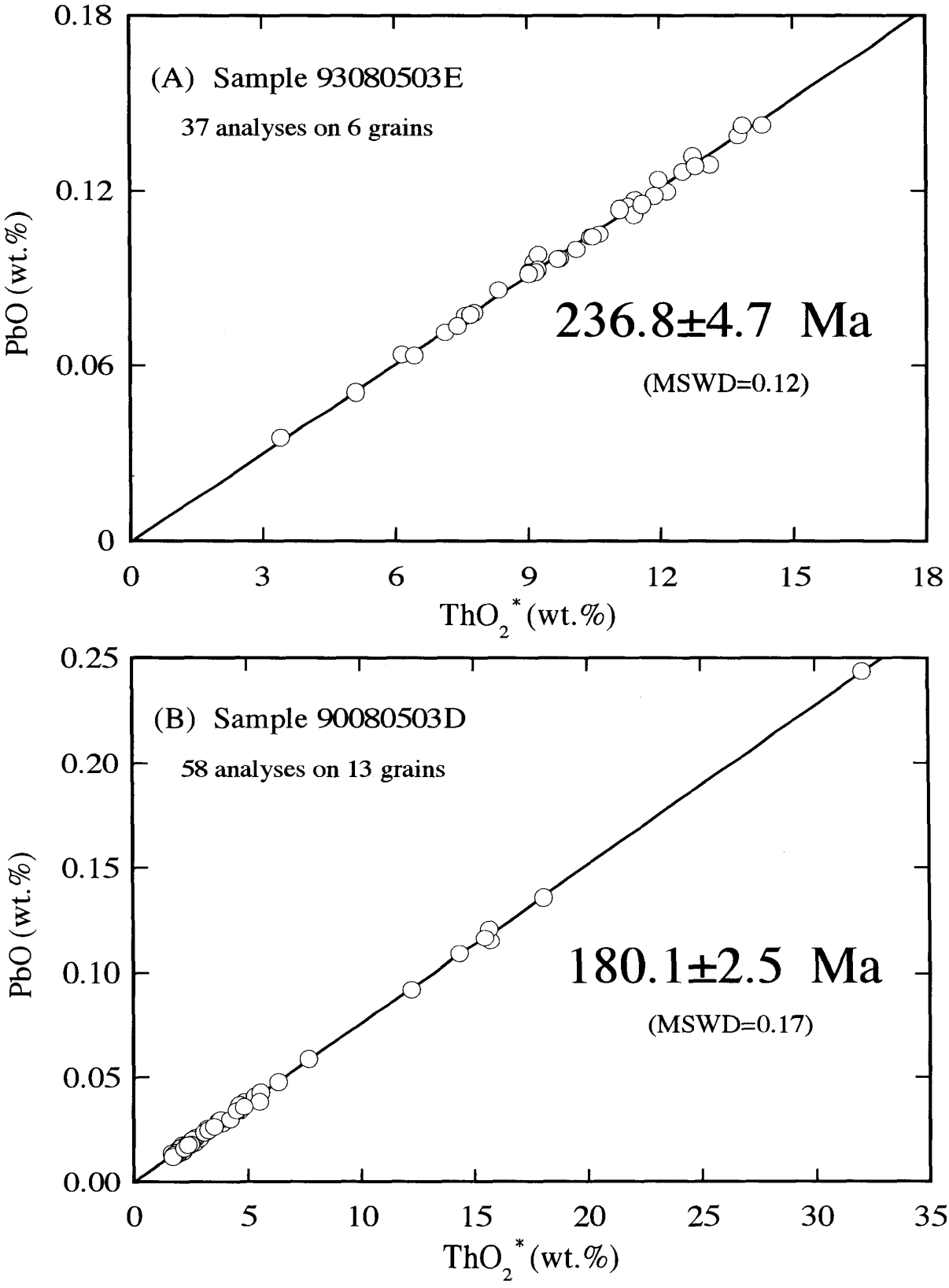

Fig. 5. Plots of PbO vs. ThO_2* of monazite grains from the Mizunashi Granite (A) and a pegmatite vein (B). The error given to the age calculation is of 2σ.

Pegmatite vein (Sample 93080503D)

A total of 58 spots on transparent portions of 13 monazite grains were analyzed. The ThO_2* content varies from 1.71 to 32.0%, and the PbO content from 0.012 to 0.244%. The apparent ages for individual spots are in the range between 169 and 196 Ma. The PbO-ThO_2* plots of 58 data are given in Fig. 5B. The regression line, having a slope of 0.0076 ± 0.0001 and an intercept value of -0.0001 ± 0.0004, yields an age of 180.1 ± 2.5 Ma (MSWD = 0.17).

DISCUSSION

The CHIME monazite ages for samples of the Hida Gneiss, 250.5 ± 6.8 and 248.9 ± 4.5 Ma, agree well with each other. The closure temperature of Pb diffusion in monazite is 650–700°C (Suzuki et al., 1994). Smith and Barreiro (1970) found that monazite in gneisses formed as metamorphic mineral at the lower amphibolite facies conditions records the time since the formation even with subsequent excursions into upper amphibolite facies. The stable association of muscovite and quartz shows that the gneiss samples did not experience the upper amphibolite facies conditions. We thus consider that the ca. 250 Ma monazite ages date the first attainment to the lower amphibolite facies grade during the prograde stage of the Hida metamorphism.

If the Hida Gneiss is of polymetamorphosed Precambrian origin as has been speculated previously, monazite grains should bear signature of older ages. Despite our search for Precambrian monazite cores over 29 grains from sample 90080502A and 46 grains from sample 90080502B, no parts older than ca. 250 Ma have been found. Suzuki and Adachi (1994) reported the occurrence of ca. 350 Ma detrital zircons from psammitic gneiss samples in the Tsunokawa area, east of the Amo area. This indicates that sedimentation of the gneiss protolith took place in the middle-late Paleozoic. Again, we can state that the Hida metamorphic rocks in the Amo area formed in the late Permian, and are not polymetamorphosed Precambrian rocks.

The CHIME monazite age of the Mizunashi Granite is 236.8 ± 4.7 Ma. This age is slightly younger than the previously reported Rb-Sr whole-rock isochron age of 296.7 ± 25.6 Ma (Shibata and Nozawa, 1984). Since the Rb-Sr isotopic data are scattered, we here regard the 236.8 ± 4.7 Ma age as the time of granite emplacement. Another Rb-Sr mineral isochron age for the Mizunashi Granite was reported as 210.9 ± 1.8 Ma (Shibata and Nozawa, 1984). This age is evidently older than the age for the post-tectonic Funatsu granitic rocks (188.9 ± 4.4 Ma; Shibata and Nozawa, 1984), and is correlatable with K-Ar hornblende and muscovite ages for the Hida Gneiss. Therefore, it seems much more likely that the Mizunashi Granite was emplaced possibly at the peak metamorphism and cooled together with the Hida Gneiss to the blocking temperatures of hornblende and muscovite at ca. 210 Ma.

The CHIME monazite age of 180.1 ± 2.5 Ma for the pegmatite vein cutting the Mizunashi Granite is correlative with the 188.9 ± 4.4 Ma Rb-Sr whole-rock isochron age of the Funatsu granitic rocks (Shibata and Nozawa, 1984). Probably

the pegmatite vein had been derived from the late stage residual of the Funatsu granitic rocks.

CONCLUDING REMARKS

The CHIME ages of monazite have revealed that the Hida Gneiss in the Amo area originated from late Paleozoic sediments and attained at the lower amphibolite facies grade in late Permian time (ca. 250 Ma). The peak metamorphism was possibly contemporaneous with the emplacement of the Mizunashi Granite at ca. 237 Ma. Taking available K-Ar and Rb-Sr mineral ages into consideration, we can conclude that both the gneisses and granite cooled to blocking temperature of hornblende and muscovite at ca. 210 Ma. The Hida Gneiss and the Mizunashi Granite subsequently underwent the intrusion of pegmatite at ca. 180 Ma. The previous view that Hida metamorphic rocks formed in Precambrian time is no longer valid.

ACKNOWLEDGEMENTS

We thank Mr. S. Yogo of Nagoya University for his technical assistance and anonymous reviewers for their constructive comments. One of the authors (I. H. Khan) wishes to express his profound thanks to Japan International Cooperation Agency for providing an opportunity for his research, and is indebted to JICA and Department of Earth and Planetary Sciences, Nagoya University. The coordinating and arranging effort of Dr. T. Shirahase, JICA Expert for Geoscience Laboratory and Dr. N. Fujii, Director of Applied Geology, Tamano Consultant Co. Ltd. are also thanked.

REFERENCES

Adachi, M. and Suzuki, K. (1992) A preliminary note on the age of detrital monazites and zircons from sandstones in the Upper Triassic Nabae Group, Maizuru terrane. *Mem. Geol. Soc. Japan*, **38**, 111–120.

Hiroi, Y. (1981) Subdivision of the Hida metamorphic complex, central Japan, and its bearing on the geology of the Far East in Pre-Sea of Japan time. *Tectonophysics*, **76**, 317–333.

Minato, M., Gorai, M. and Funahashi, M. (1965) The geologic development of the Japanese Islands. *Tsukiji Shokan Com.*, 442pp.

Nozawa, T., Kawada, K. and Kawai, M. (1975) Geology of the Hida-Furukawa District. Quadrangle Series, scale 1:50,000, Geol. *Surv. Japan*, 79pp.

Ota, K. and Itaya, T. (1989) Radiometric ages of granitic and metamorphic rocks in the Hida metamorphic belt, central Japan. *Bull. Hiruzen Res. Inst., Okayama University of Science*, no.**15**, 1–25.

Sato, S. (1968) Precambrian-Variscan polymetamorphism in the Hida massif, basement of the Japanese Islands. *Sci. Rept. Tokyo Univ. Educ., Sec. C*, **10**, 15–129.

Sato, S., Shirahase, T. and Shibata, H. (1967) Older granite based on the Rb-Sr dating in the Hida massif. *Jour. Geol. Soc. Japan*, **73**, 72.

Shibata, K. and Nozawa, T. (1984) Isotopic ages of the Funatsu Granitic Rocks. *J. Japan. Assoc. Min. Pet. Econ. Geol.*, **79**, 289–298.

Shibata, K. and Nozawa, T. (1986) Late Precambrian ages for granitic rocks intruding the Hida Metamorphic Rocks. *Bull. Geol. Surv. Japan*, **37**, 43–51.

Shibata, K., Nozawa, T. and Wanless, R.K. (1970) Rb-Sr geochronology of the Hida metamorphic belt, Japan. *Can. Jour. Earth Sic.*, **7**, 1383–1401.

Shibata, K., Kano, T. and Asano, M. (1989) Isotopic ages of the Gray granite from the upper Kubusu River area, Hida Mountains. *J. Min. Pet. Econ. Geol.*, **84**, 243–251.

Smellie, J.A.T., Cogger, N. and Herrington, J. (1978) Standards for quantitative microprobe determination of uranium and thorium with additional information on the chemical formulate of davidite and euxenite-polycrase. *Chem. Geol.*, **22**, 1–10.

Smith, H.A. and Barreiro, B. (1990) Monazite U-Pb dating of staurolite grade metamorphism in pelitic schists. *Contrib. Mineral. Petrol.*, **105**, 602–615.

Suwa, K. (1969) Polymetamorphism in the Hida metamorphic complex. *Mem. Geol. Soc. Japan*, no.**4**, 113–116.

Suwa, K. (1990) Hida-Oki terrane. Pre-Cretaceous terranes of Japan. Edited by K. Ichikawa, S. Mizutani, I. Hara, S. Hada and A. Yao, Publication of IGCP Project 224, 13–24.

Suzuki, M. (1977) Polymetamorphism in the Hida Metamorphic Belt, central Japan. *Jour. Sci. Hiroshima Univ.*, **7**, 217–296.

Suzuki, K. and Adachi, M. (1991a) Precambrian provenance and Silurian metamorphism of the Tsubonosawa paragneiss in the South Kitakami terrane, Northeast Japan, revealed by the chemical Th-U-total Pb isochron ages of monazite, zircon and xenotime. *Geochem. J.*, **25**, 357–376.

Suzuki, K. and Adachi, M. (1991b) The chemical Th-U-total Pb isochron ages of zircon and monazite from the Gray Granite of the Hida terrane, Japan. *J. Earth Sci., Nagoya Univ.*, **38**, 11–38.

Suzuki, K. and Adachi, M. (1994) Middle Precambrian detrital monazite and zircon from the Hida gneiss on Oki-Dogo Island, Japan: their origin and implications for the correlation of basement gneiss of Southwest Japan and Korea. *Tectonophysics*, **235**, 277–292.

Suzuki, K., Adachi, M. and Kajizuka, I. (1994) Electron microprobe observations of Pb diffusion in metamorphosed detrital monazites. *Earth Planet. Sci. Lett.*, **128**, 391–405.

Suzuki, K., Adachi, M. and Tanaka, T. (1991) Middle Precambrian provenance of Jurassic sandstone in the Mino terrane, central Japan: Th-U-total Pb evidence from an electron microprobe monazite study. *Sediment. Geol.*, **75**, 141–147.

Suzuki, K., Adachi, M., Sango, K. and Chiba, H. (1992) Chemical Th-U-total Pb isochron ages of monazites and zircons from the Hikami Granite and "Siluro-Devonian" clastic rocks in the South Kitakami terrane. *J. Min. Pet. Econ. Geol.*, **87**, 330–349.